PROCEEDINGS OF SCIENCE

Recent triboson results from the CMS and ATLAS experiments

Ying An*on behalf of the ATLAS and CMS Collaborations

*Peking University, School of Physics, Beijing, China

E-mail: ying.an@cern.ch

The latest triboson results in LHC proton-proton collisions at a center-of-mass energy of 13 TeV are presented. The full Run 2 data collected from 2016 to 2018 and recorded by the CMS and ATLAS detectors corresponding to integrated luminosities of 137 and 139 fb^{-1} are used, respectively. Triboson processes containing photons (V$\gamma\gamma$) and without any photons are included, where V=W, Z. Exclusion limits on anomalous quartic gauge couplings based on the dimension eight operators of the effective field theory are derived at 95% confidence level in measurements of V$\gamma\gamma$ production.

The Tenth Annual Conference on Large Hadron Collider Physics - LHCP2022
16-20 May 2022
online

*Speaker

https://pos.sissa.it/

PoS(LHCP2022)176

1. Introduction

The triboson production measurement is only feasible at the LHC with enough statistics to perform a precise measurement. There are multiboson coupling vertices having both Standard Model (SM) and Beyond SM theory predictions. Any deviations from the SM predictions would provide hints for new physics at a higher energy scale which is presently inaccessible [1–6]. Moreover, the Higgs boson can also play a role in the production. These all make the corresponding studies at the ATLAS and CMS experiments interesting.

2. Triboson measurements containing photons

The triboson production of a W or Z boson in association with two photons is measured by the CMS experiment [7, 8]. The fully leptonic decays W$\to \ell\nu$ and Z$\to \ell\ell$, where ℓ = e or μ, are used to select events of interest. At least two photons are required. Furthermore, the separation of the two photons, and between photons and leptons, should satisfy $\Delta R > 0.4$, where $\Delta R = \sqrt{(\Delta\eta)^2 + (\Delta\phi)^2}$.

The main backgrounds come from the misidentification of jets and electrons as photons. Another contribution is from processes containing real photons from top quark production in association with photons and the production of massive gauge boson plus photons, which has a small contribution. The nonprompt photon background is estimated in a Vγ control region in which two kinds of photons are defined as tight or loose by different requirements on isolation [9, 10]. Assuming ϵ and f are probabilities of tight photon and jet calculated by the simulation and data, the nonprompt photon contribution should follow Eq 1, where α represents the number of background events derived from data, and the subscript index represents the leading or trailing photon. The correctness of this contribution is validated in the control region seen in Fig. 1 (right). The contribution of electrons misidentified as a photon is estimated by the fit in data and simulation using an invariant mass of an electron and a photon in Zγ events. A correction factor defined as $\mathcal{F}(p_{\mathrm{T}},\eta) = \frac{N_{\mathrm{inv}}^{\mathrm{data}}/N_{\mathrm{Z}}^{\mathrm{data}}}{N_{\mathrm{inv}}^{\mathrm{MC}}/N_{\mathrm{Z}}^{\mathrm{MC}}}$ is then computed, where $N_{\mathrm{inv}}^{\mathrm{data\,(MC)}}$ and $N_{\mathrm{Z}}^{\mathrm{data\,(MC)}}$ in the numerator (denominator) are the number of events derived from the fit using either signal shape or double-sided Crystal-Ball function [11] in data (simulation).

$$N_{\mathrm{TT}}^{\mathrm{j}\to\gamma} = \sum\nolimits_{(p_{\mathrm{T}},\eta)_{\gamma1}\,(p_{\mathrm{T}},\eta)_{\gamma2}} (\epsilon_1 f_2 \alpha_{\gamma\mathrm{j}} + f_1\epsilon_2\alpha_{\mathrm{j}\gamma} + f_1 f_2 \alpha_{\mathrm{jj}}). \tag{1}$$

The signal strength, significance, and limits on anomalous quartic gauge couplings are extracted in bins of $p_{\mathrm{T}}^{\gamma\gamma}$ via maximum likelihood fits [12]. After the fits, the observed (expected) significance for the W$\gamma\gamma$ signal in the combined channels is 3.1 (4.5) σ; for the Z$\gamma\gamma$ in the muon channel is 5.4 (5.1) σ and 4.8 (5.8) σ in the combined channels. The signal strengths are $\mu_{\mathrm{WW}\gamma} = 0.73\,^{+0.10}_{-0.10}\,(\mathrm{stat})\,^{+0.22}_{-0.22}\,(\mathrm{syst})$ and $\mu_{\mathrm{ZZ}\gamma} = 0.91\,^{+0.10}_{-0.09}\,(\mathrm{stat})\,^{+0.11}_{-0.12}\,(\mathrm{syst})$. The limits on the dimension eight operators [13] M_{2-3}, T_{0-2}, and T_{5-7} based on the effective theory [14] for W$\gamma\gamma$ channel and the T_{0-2} and T_{5-9} operators for Z$\gamma\gamma$ are derived at 95% confidence level. The post-fit distributions of $p_{\mathrm{T}}^{\gamma\gamma}$ and the yields in the presence of the anomalous coupling parameter $f_{\mathrm{T0}}/\Lambda^4$ set to be 10 TeV^{-4} are shown in Fig. 1 (left).

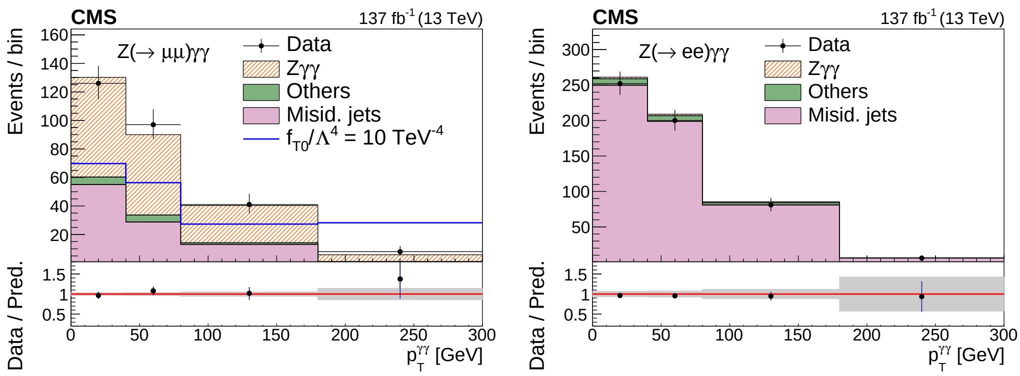

Figure 1: Distributions of the transverse momentum of the diphoton system for the $Z\gamma\gamma$ muon channel in the signal region (left) and a nonprompt photon control region (right). The blue line represents a nonzero f_{T0}/Λ^4 value enhancing the yields at high $p_T^{\gamma\gamma}$ [8].

3. Triboson measurements of three massive vector bosons

The measurement of triboson VVV production, V= W, Z, has been observed by both the CMS [15] and ATLAS [16, 17] Collaborations. In the results of the ATLAS experiment, the WWW process is measured and constitutes the first observation. In the results of the CMS experiment, the WWW, WWZ, WZZ, and ZZZ channels are measured separately and then combined to give the first observation of the VVV process. The main backgrounds in this VVV analysis are the lost-lepton contribution from the diboson process, from jets misidentified as leptons[18], Vγ process where the photon is misidentified as an electron, the lepton charge flip contribution, and other backgrounds with small yields including the production of $t\bar{t}$ in association with a boson.

In the ATLAS $W^{\pm}W^{\pm}W^{\mp}$ measurement, the final states of $\ell^{\pm}\ell^{\pm}jjp_T^{miss}$ and $\ell^{\pm}\ell^{\pm}\ell^{\mp}$ are exploited, where the former corresponds to the categories of $e^{\pm}e^{\pm}$, $\mu^{\pm}\mu^{\pm}$, and $e^{\pm}\mu^{\pm}$, but the latter corresponds to the categories of $e^{\pm}e^{\pm}\mu^{\mp}$ and $\mu^{\pm}\mu^{\pm}e^{\mp}$ discarding the cases having pairs of opposite-sign same-flavor (OSSF) leptons to decrease the contribution from Z bosons. To select the 2ℓ signal, the requirements of $m_{jj} < 160$ GeV, $N_j \geq 2$, $|\Delta\eta_{jj}| < 1.5$ are applied to reject the contribution from vector boson scattering processes (VBS). The requirements of $40 < m_{\ell\ell} < 400$ GeV, $m_{ee} < (>) 80\,(100)$ GeV, $E_T^{significance} > 3$ [19] and no jets from b-quarks (b) are utilized to reduce nonprompt backgrounds. In the 3ℓ signal region, no b-jets and sum of lepton charge requirements are applied. The dominant background from the WZ process with 0-2 jets is normalized by data events in the corresponding three WZ-enriched control regions. Besides, other control regions enriched in $t\bar{t}$, $Z\gamma$, and $Z\to ee$ [18] are built to derive factors as event weights to the data-driven samples of nonpromt lepton, misidentified photons, and charge flip. The boosted decision trees [20] (BDTs) are trained in signal regions for the 2ℓ and 3ℓ categories to further separate the signal from backgrounds. Each BDT is trained with 11 variables and the BDT distribution is then used to build the binned likelihood [12] to extract the signal strength in a simultaneous fit of signal and WZ control regions shown in Fig. 2, which displays event yields after the fit. The observed (expected) significance is 8.2 (5.4) standard deviations (sd) corresponding to the $pp \to$ WWW cross section of $850 \pm 100(\text{stat}) \pm 80(\text{syst})$ fb.

In the measurement of VVV from CMS, besides the WWW measurement, the WWZ, WZZ,

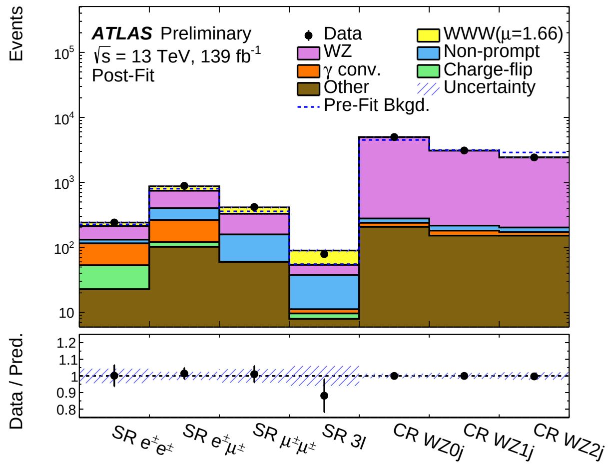

Figure 2: Post-fit event yields for data, signal, and background in the four SRs and three WZ CRs [17].

and ZZZ are also measured. For the WWW analysis, 2ℓ and 3ℓ signals are used which is the same as the ATLAS analysis, however, more cases are considered. In the 2ℓ [21] category, one case of exactly one jet and two cases with two or more jets separated by the requirements of $|m_{\rm jj} - m_{\rm W}| > 15$ GeV are included. Another two cases of 1 and 2 OSSF lepton pair(s) are added in the 3ℓ category. In total, there are 9 bins in 2ℓ and 3 bins in 3ℓ. For other VVV production, only the fully leptonic final states are considered. In the WWW analysis, instead of defining a signal region by selecting directly on discriminating features, two BDTs are trained against instrumental backgrounds [21] and real backgrounds. In the WWZ analysis, depending on the combination of W boson decays, there are categories of ee/$\mu\mu$ and eμ. Two BDTs are trained to separate the eμ signal against the ZZ and $t\bar{t}$Z backgrounds. One BDT is trained for ee/$\mu\mu$ against ZZ. In total, seven bins are used. In the WZZ and ZZZ analysis, because of the small cross sections and branching ratio of the fully leptonic decay, a BDT method is not used, and instead, a single selection is applied for each process, resulting in one bin for each. Finally, the signal strength (μ) is determined through simultaneous fits in all 21 signal bins shown in Fig. 3 (right) with either four independent μ for the four processes separately or one $\mu_{\rm comb}$ for all VVV channels combined. Results are shown in Fig. 3 (left). The significance of the observation is 5.7 sd with 5.9 sd expected.

4. Conclusions

The most recent triboson results from the CMS and ATLAS experiments at the LHC are discussed. The CMS Collaboration reports the first observation of the combined production of three massive gauge bosons. Besides the VVV measurements, CMS also provides the results of the V$\gamma\gamma$ measurement. The ATLAS Collaboration provides the first observation of WWW production with the cross section of 850 ± 100(stat) ± 80(syst) fb which is approximately 2.6 sd from the predicted cross section of 511 ± 18 fb calculated at NLO QCD and LO electroweak accuracy [22–25].

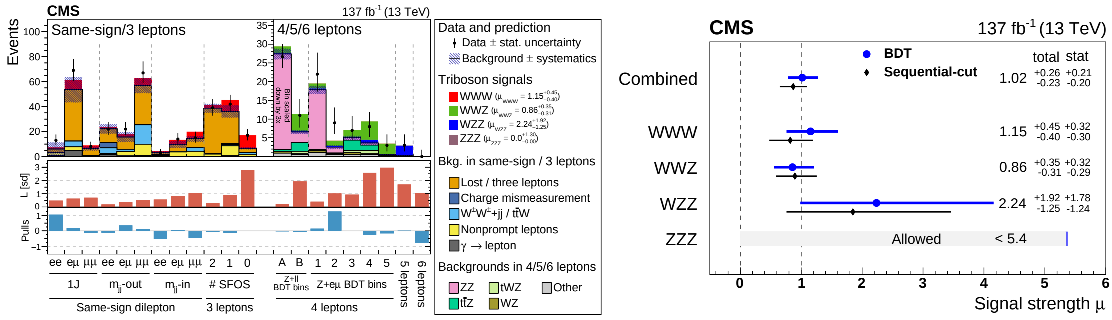

Figure 3: Comparison of the observed numbers of events to the predicted yields after fitting (left) and best-fit values of the signal strengths (right) for the BDT-based analyses (blue solid circles) and the sequential-cut analyses (black open circles) [15].

References

[1] H.-Y. Ren, L.-H. Xia and Y.-P. Kuang, *Model-independent Probe of anomalous heavy neutral Higgs bosons at the LHC*, *Phys. Rev. D* **90** (2014) 115002 [1404.6367].

[2] Y.-P. Kuang, H.-Y. Ren and L.-H. Xia, *Further investigation of the model-independent probe of heavy neutral Higgs bosons at LHC Run 2*, *Chin. Phys. C* **40** (2016) 023101 [1506.08007].

[3] K. Agashe, P. Du, S. Hong and R. Sundrum, *Flavor Universal Resonances and Warped Gravity*, *JHEP* **01** (2017) 016 [1608.00526].

[4] K.S. Agashe, J. Collins, P. Du, S. Hong, D. Kim and R.K. Mishra, *LHC Signals from Cascade Decays of Warped Vector Resonances*, *JHEP* **05** (2017) 078 [1612.00047].

[5] K. Agashe, J.H. Collins, P. Du, S. Hong, D. Kim and R.K. Mishra, *Dedicated Strategies for Triboson Signals from Cascade Decays of Vector Resonances*, *Phys. Rev. D* **99** (2019) 075016 [1711.09920].

[6] J.A. Aguilar-Saavedra, *Profile of multiboson signals*, *JHEP* **05** (2017) 066 [1703.06153].

[7] CMS Collaboration, *The CMS Experiment at the CERN LHC*, *JINST* **3** (2008) S08004.

[8] CMS Collaboration, *Measurements of the $pp \to W^{\pm}\gamma\gamma$ and $pp \to Z\gamma\gamma$ cross sections at $\sqrt{s}$ = 13 TeV and limits on anomalous quartic gauge couplings*, *JHEP* **10** (2021) 174 [2105.12780].

[9] ATLAS Collaboration, *Measurements of $Z\gamma$ and $Z\gamma\gamma$ production in pp collisions at $\sqrt{s} = 8$ TeV with the ATLAS detector*, *Phys. Rev. D* **93** (2016) 112002.

[10] CMS Collaboration, *Measurements of the $pp \to W\gamma\gamma$ and $pp \to Z\gamma\gamma$ cross sections and limits on anomalous quartic gauge couplings at $\sqrt{s}$ = 8 TeV*, *JHEP* **10** (2017) 072 [1704.00366].

[11] M.J. Oreglia, *A study of the reactions* $\psi' \to \gamma\gamma\psi$, Ph.D. thesis, Stanford University, 1980, http://www.slac.stanford.edu/cgi-wrap/getdoc/slac-r-236.pdf.

[12] G. Cowan, K. Cranmer, E. Gross and O. Vitells, *Asymptotic formulae for likelihood-based tests of new physics*, *Eur. Phys. J. C* **71** (2011) 1554 [1007.1727].

[13] O.J.P. Éboli, M.C. Gonzalez-Garcia and J.K. Mizukoshi, *$pp \to jje^{\pm}\mu^{\pm}\nu\nu$ and $jje^{\pm}\mu^{\mp}\nu\nu$ at $O(\alpha_{em}^6)$ and $O(\alpha_{em}^4\,\alpha_s^2)$ for the study of the quartic electroweak gauge boson vertex at CERN LHC*, *Phys. Rev. D* **74** (2006) 073005 [hep-ph/0606118].

[14] C. Degrande, N. Greiner, W. Kilian, O. Mattelaer, H. Mebane, T. Stelzer et al., *Effective Field Theory: A Modern Approach to Anomalous Couplings*, *Annals Phys.* **335** (2013) 21 [1205.4231].

[15] CMS Collaboration, *Observation of the Production of Three Massive Gauge Bosons at $\sqrt{s}$ =13 TeV*, *Phys. Rev. Lett.* **125** (2020) 151802 [2006.11191].

[16] ATLAS Collaboration, *The ATLAS Experiment at the CERN Large Hadron Collider*, *JINST* **3** (2008) S08003.

[17] ATLAS Collaboration, *Observation of WWW production in pp collisions at $\sqrt{s} = 13$ TeV with the ATLAS detector*, *Phys. Rev. Lett.* **129** (2022) 061803 [2201.13045].

[18] ATLAS Collaboration, *Measurement of $W^{\pm}W^{\pm}$ vector-boson scattering and limits on anomalous quartic gauge couplings with the ATLAS detector*, *Phys. Rev. D* **96** (2017) 012007 [1611.02428].

[19] ATLAS Collaboration, *Performance of missing transverse momentum reconstruction with the ATLAS detector using proton-proton collisions at $\sqrt{s} = 13$ TeV*, *Eur. Phys. J. C* **78** (2018) 903 [1802.08168].

[20] T. Chen and C. Guestrin, *Xgboost: A scalable tree boosting system*, KDD '16, (New York, NY, USA), p. 785–794, Association for Computing Machinery, 2016, DOI.

[21] CMS Collaboration, *Search for the production of $W^{\pm}W^{\pm}W^{\mp}$ events at $\sqrt{s} = 13$ TeV*, *Phys. Rev. D* **100** (2019) 012004 [1905.04246].

[22] Y.-B. Shen, R.-Y. Zhang, W.-G. Ma, X.-Z. Li and L. Guo, *NLO QCD and electroweak corrections to WWW production at the LHC*, *Phys. Rev. D* **95** (2017) 073005 [1605.00554].

[23] S. Dittmaier, G. Knippen and C. Schwan, *Next-to-leading-order QCD and electroweak corrections to triple-W production with leptonic decays at the LHC*, *JHEP* **02** (2020) 003 [1912.04117].

[24] S. Dittmaier, A. Huss and G. Knippen, *Next-to-leading-order QCD and electroweak corrections to WWW production at proton-proton colliders*, *JHEP* **09** (2017) 034 [1705.03722].

PoS(LHCP2022)176

[25] C. Anastasiou, C. Duhr, F. Dulat, E. Furlan, T. Gehrmann, F. Herzog et al., *High precision determination of the gluon fusion Higgs boson cross-section at the LHC*, *JHEP* **05** (2016) 058 [1602.00695].